

This work was written as part of one of the author's official duties as an Employee of the United States Government and is therefore a work of the United States Government. In accordance with 17 U.S.C. 105, no copyright protection is available for such works under U.S. Law.

Public Domain Mark 1.0

<https://creativecommons.org/publicdomain/mark/1.0/>

Access to this work was provided by the University of Maryland, Baltimore County (UMBC) ScholarWorks@UMBC digital repository on the Maryland Shared Open Access (MD-SOAR) platform.

Please provide feedback

Please support the ScholarWorks@UMBC repository by emailing scholarworks-group@umbc.edu and telling us what having access to this work means to you and why it's important to you. Thank you.

Goddard UV aerosol absorption closure experiment (2002-03)

N.A. Krotkov^{*a}, P.K. Bhartia^b and J.R.Herman^b, Jim Slusser^d,
Gwen Scott^d, G. Labow^c, A. Vasilkov^c, T. Eck^a, O. Dubovik^a, and B. Holben^b

^aGoddard Earth Sciences and Technology Center Univ. of Maryland Baltimore County, MD USA;

^bNASA Goddard Space Flight Center, Greenbelt, MD USA;

^cScience Systems and Applications, Inc., Lanham, MD USA 20706

^dUSDA UVB Monitoring Network and Colorado State University

ABSTRACT

Compared to the visible spectral region very little is known about aerosol absorption in UV. Without such information it is impossible to quantify a cause to the observed discrepancy between modeled and measured UV irradiances and photolysis rates. We report preliminary results of an aerosol closure experiment where a UV-shadow-band radiometer (UVMFRSR, USDA UVB Monitoring and Research Network) and well-calibrated sun-sky radiometer (CIMEL, NASA AERONET network) were run side-by-side for several months at NASA/GSFC site in Greenbelt, MD. The aerosol optical thickness, τ , was measured at 340nm and 380nm by the CIMEL direct-sun technique. These results compared well with independent MFRSR τ measurements at 368nm (using total minus diffuse irradiance technique). Such comparisons provide an independent check of both instrument's radiometric and MFRSR's angular calibration and allow precise tracking of the UV filter degradation by repeating the comparisons made at somewhat regular time intervals. The τ measurements were used as input to a radiative transfer model along with AERONET retrievals of the column-integrated particle size distribution (PSD) to infer an effective imaginary part of the UV aerosol refractive index (k). This was done by fitting the MFRSR diffuse fraction measurements to the calculated values for each UV spectral channel. Inferred values of refractive index and PSD allow calculation of the single scattering albedo, ω , in the UV and comparisons with AERONET ω retrievals. The advantage of utilizing diffuse fraction measurements is that radiometric calibration is not needed for the MFRSR since the same detector measures both the total and diffuse flux. The additional advantage is that surface albedo is much smaller in the UV than in the visible spectral range and has much less effect on aerosol measurements.

Keywords: ultraviolet radiation, aerosol absorption, single scattering albedo, CIMEL sun photometer, AERONET network, UV multi-filter rotating shadow band radiometer, UV MFRSR, diffuse fraction measurements

1. INTRODUCTION

The knowledge of aerosol absorption in the near UV is of interest to tropospheric chemistry because it changes the rate of photochemical reactions^{1,2} and smog production³ as well as penetration of biologically harmful UV radiation to the surface⁴⁻¹³. However, such properties of aerosol absorbers in the UV are poorly known, which makes it difficult to quantify a cause to the observed discrepancy in modeled and measured UV irradiances¹⁴ and photolysis rates. We report preliminary results of an aerosol closure experiment where UV-shadow-band radiometer (UVMFRSR, USDA UVB Monitoring and Research Network)¹⁵⁻¹⁷ and well-calibrated sun-sky radiometer (CIMEL, NASA AERONET network)^{18,19} were run side-by-side for several months at NASA/GSFC site in Greenbelt, MD. We first compare aerosol optical thickness, τ , measurements by both techniques. Next, MFRSR τ measurements were used as input to a radiative transfer model along with AERONET retrievals of the column-integrated particle size distribution (PSD) and real part of effective refractive index to infer an effective imaginary part of the UV aerosol refractive index (k)²⁰⁻²⁴.

* Krotkov@chescat.gsfc.nasa.gov; phone 1 301 614-5553; fax 1 301 614-5903; <http://toms.gsfc.nasa.gov>; GEST Center, NASA/GSFC Code 916 Greenbelt, Maryland 20771

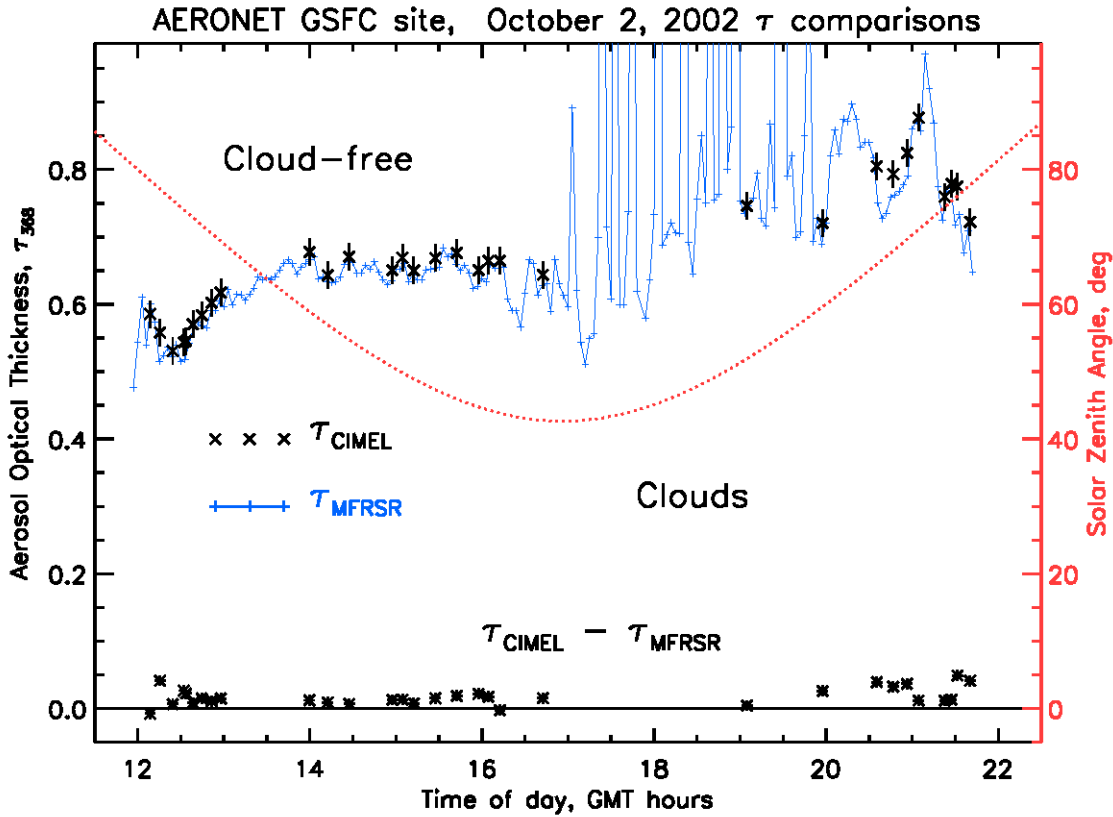


Figure 1. Left axis show aerosol optical thickness data on October 2 2002. Small crosses connected with solid line show MFRSR τ_{368} derived from the difference between total and diffuse irradiance. Large crosses with ± 0.02 error bars show τ_{368} interpolated from co-located and simultaneous CIMEL direct sun τ measurements at 340nm and 380nm. The dashed curve shows solar zenith angle variation during the day (right axis). The absolute differences between CIMEL and UVMFRSR τ measurements are shown as stars at the bottom of the figure. The daily mean bias between two instruments ($+0.018$) is within reported errors²⁶ for CIMEL τ measurement in UV. The standard deviation of the difference ($\sigma_{\tau \text{ difference}} = 0.013$) is much less than τ variability on that day: $\sigma_{\tau} = 0.09$.

Inferred values of k and PSD allow calculation of the single scattering albedo ω in the UV and comparisons with AERONET ω retrievals at visible wavelengths²⁵⁻²⁷.

2. DATA SETS

The UV-MFRSR is a shadow-band instrument that measures diffuse and total horizontal radiation¹⁶. The USDA UVB Monitoring and Research Network operates 31 of these instruments continuously¹⁵. These instruments are capable of retrieving column ozone²⁸, aerosol optical depth¹⁷ and the diffuse to direct irradiance ratio. The radiometric stability these instruments is about $\pm 2\%$ to 5% per year based on numerous calibrations performed at the NOAA Central UV Calibration Facility in Boulder. UV-MFRSR instrument was installed at the AERONET primary calibration site at NASA Goddard Space Flight Center (GSFC) by the USDA UVB network with routine operation started on October 1, 2002. The instrument's location on an elevated platform on the roof of a building allows an unobstructed view of the horizon. Special attention was given to properly leveling-off the instrument.

The raw data were automatically transmitted (via dedicated telephone modem) to USDA network processing center for calibration and further processing by UVB network. Figure 1 shows MFRSR derived 368nm aerosol optical thickness,

τ_a data taken at 3 min time intervals on October 2, 2002. The spikes in measured τ_a between 17GMT and 20GMT result mainly from scattered clouds blocking direct solar irradiance. Therefore, automatic cloud screening procedure needs yet to be developed for MFRSR routine operation.

CIMEL Electronique CE-318 Sun-sky radiometer measurements were made with reference (master) instruments of the AERONET global network¹⁸. The automatic tracking Sun and sky scanning radiometers made direct sun measurements with a 1.2° full field of view every 15 minute at 340, 380, 440, 500, 675, 870, 940 and 1020nm. The CIMEL derived τ_a at GSFC on October 2, 2002 is also shown in Figure 1. For comparisons with MFRSR τ_a measurements at 368nm, CIMEL τ_a data were interpolated linearly between 340nm and 380nm on a log-log scale. These results compared well with independent MFRSR τ measurements. We note that (a) the absolute τ_a differences are within specified AERONET uncertainty (± 0.02)^{19,29} throughout the day and (b) both instruments track each other with uniform high precision, despite cloud interference in the afternoon. This proves that scattered clouds do not considerably affect MFRSR τ_a measurements provided they do not block the sun.

We also did not observe diurnal variation in τ_a difference with solar zenith angle (shown on right hand side of the plot). This proves that cosine correction of the MFRSR derived normal direct irradiance is reliable up to solar zenith angle 80°.

This good agreement in τ_a is typical throughout whole intercomparison period at GSFC and provides confidence in UV aerosol single scattering albedo retrievals (see below). Such comparisons provide independent check on both instrument's radiometric and MFRSR's angular calibration and allow precise tracking of the UV filter degradation by repeating the comparisons made at somewhat regular time intervals.

Almucantar sky radiance measurements were also made by the CIMEL instruments on relatively cloud-free periods at optical air masses of 4, 3, 2 in the morning and afternoon, and once per hour in between. We used cloud-screened³⁰ CIMEL sky radiance almucantar measurements at 440nm, 675nm, 870nm and 1020nm in conjunction with the direct sun-measured aerosol optical thickness τ_a at these wavelengths to retrieve column average aerosol size distribution, PSD and effective refractive index (real and imaginary part independently at each wavelength) following the methodology of Dubovik and King²⁵. Internally homogeneous spherical particles with radii between 0.05 and 15 micron were assumed in the retrievals of PSD and effective refractive index. The refractive index was not allowed to vary with particle radius and the strict boundaries were set on the real part of the refractive index (between 1.33 and 1.6). Thus, the inversion allows estimation of spectral single scattering albedo, ω , between 440 and 1020nm with an uncertainty of ~ 0.03 depending on aerosol type and optical depth^{26,27}.

3. METHODOLOGY OF MFRSR AEROSOL SINGLE SCATTERING ALBEDO RETRIEVAL

MFRSR ozone and τ measurements at 325nm, 332nm and 368nm were used as input to University of Arizona vector radiative transfer model³¹ along with AERONET standard retrievals of the column-integrated particle size distribution, PSD and real part of refractive index at 440nm (<http://aeronet.gsfc.nasa.gov>) to infer an effective imaginary part of the UV aerosol refractive index (k). This was done by fitting the MFRSR diffuse fraction measurements to the calculated values separately for each MFRSR UVA spectral channel. The MFRSR slit averaged cross sections along with SUSIM extraterrestrial solar flux data are given in Table 1. The advantage of utilizing diffuse-fraction measurements is that radiometric calibration is not needed for the MFRSR, since the same detector measures both the total and diffuse flux.

The AERONET PSD changes not only from day to day, but also during single day. Since a complete set of CIMEL almucantar measurements at 4 wavelengths takes about 5 minutes (and τ_a from ± 16 minutes are used as input to the inversion), while MFRSR measurements were made at 3-minute intervals, we have analyzed all available MFRSR data within time interval ± 20 min of each AERONET almucantar measurement.

Table 1 Effective cross-sections used in Radiative transfer calculations of MFRSR total and diffuse irradiance. Rectangular slit function was assumed with FWHM=2nm. Satellite high resolution SUSIM extraterrestrial solar irradiance (ETS) data were also slit averaged

lambda(vac)	oz0	oz1	oz2	Rayleigh	Depol	ETS
nm		1/atm_cm		1/atm		[W/ (m2 nm)]
325	3.4502e-01	1.3702e-03	7.4157e-06	8.6143e-01	3.0897e-02	8.7640e-01
332	1.1387e-01	7.2309e-04	3.5074e-06	7.8732e-01	3.0600e-02	9.8988e-01
368	5.3864e-04	1.6004e-05	2.1301e-07	5.0993e-01	3.0100e-02	1.1762e+00

We assume that aerosol type does not change during this period and the only changes in radiation field arise from changes in solar zenith angle and aerosol optical thickness. Therefore, we use the same aerosol size distribution and real part of refractive index for any given 40 min time slot, but allowed for τ and θ_0 changes in 3-minute increments. Then we switch to the next 40-minute time slot around next available AERONET retrieval and use new aerosol-inverted parameters. If timeslots for 2 consecutive AERONET retrievals overlap, we simply repeat MFRSR fitting for all overlapping points with the new aerosol parameters. This approach prevents us from using of any kind of pre-calculated aerosol lookup tables. Instead, we run forward RT calculations in real time to fit every single 3-minute MFRSR diffuse fraction measurement independently at each wavelength (325nm, 332nm, 368nm). The advantage of this approach is that forward RT calculations are always done for exact conditions of the measurement (solar zenith angle, τ , aerosol parameters), so no interpolation in solar angle or aerosol parameters (other than absorption coefficient) is involved.

The methodology of forward RT modeling and MFRSR ω retrieval is as follows:

- 1) Standard discrete AERONET column volume PSD in 22 size bins between 0.05 μ m and 15 μ m was first parameterized using bi-modal lognormal volume size distribution²⁷. This parameterization requires 6 input parameters: column volume, modal radius and standard deviation separately for fine and coarse modes.
- 2) Volume PSD parameters were analytically converted to number column density parameters. Since we only need the shape of the PSD and not the absolute value, only five input parameters remain: modal radii and standard deviations separately for fine and coarse modes and the ratio of the total number of particles in fine and coarse modes. The implicit normalization occurs via specifying aerosol optical thickness to be equal to MFRSR measured optical thickness in each UV channel.
- 3) Although our RT model does not require this, we assume the refractive index to be the same for fine and coarse modes (one component aerosol model) to be consistent with Dubovik and King inversion strategy²⁵. Thus, following current AERONET assumptions, we seek to retrieve single effective refractive index, which is a weighted mean of the true column average refractive index over particle size distribution.
- 4) We assume the real part of refractive index, n , to be constant with wavelength, which is set to AERONET retrieved value at 440nm. We believe this assumption will not result in large retrieval error, since calculated direct irradiance is forced to be equal to the measured one, while diffuse irradiance only weakly depends on n ^{20,21}.
- 5) Dubovik and King inversion²⁵ assume a vertically homogeneous atmosphere. This may not be a good assumption in UV spectral region, especially for strongly absorbing aerosols. Thus, in our forward model we assume an a-priori relative vertical profile of the aerosol loading, which peaks in the boundary layer. The additional assumptions are that neither aerosol PSD nor the refractive index change with altitude^{20,21}. No stratospheric aerosol is assumed. This a-priori aerosol profile could be refined later using lidar measurements at GSFC.
- 6) We assume horizontally homogeneous cloud-free atmospheric conditions. The cloud free portions of days were selected by visual examination and analysis of 3-minute irradiance series and all-sky camera images.

- 7) We use a single TOMS climatological ozone and temperature profile, which is scaled to the measured total column ozone amount for every actual MFRSR measurement. The MFRSR total ozone amount compared well with co-located Brewer ozone measurements (within 2DU or <1% on October 2 2002). We currently do not assume any gaseous absorption other than ozone.
- 8) One of the main advantages the UV spectral region offers for aerosol measurements compared to the visible region is a uniformly low value of surface albedo of a few percent for snow free terrain. Thus we have manually excluded all days with even traces of partial snow cover from the current analysis. This allows us to use TOMS-derived climatologically snow-free value of surface albedo. We assume surface albedo to be the same at 325nm, 332nm and 368nm (equal to 0.02)³².
- 9) Accurately specifying surface pressure is an important requirement for radiation modeling in the UV spectral region. Since the actual surface pressure data are not currently used in derivation of τ from MFRSR, we assume 1 standard atmosphere surface pressure for all retrievals. In the future, we plan to use actual surface pressure measurements at nearby (5 km) USDA location in Beltsville, MD reduced by 3 mbar to account for change in altitude between Beltsville location (~30m asl) and GSFC MFRSR location (roof of Bld 33, ~100m asl according to our GPS measurements).
- 10) With all the previous assumptions, only one unspecified aerosol parameter remains: the imaginary part of the aerosol refractive index, k , which determines effective column average aerosol absorption. We retrieve k at each wavelength (325nm, 332nm, 368nm) by fitting the MFRSR diffuse fraction, dd (diffuse to direct ratio) measurements to the calculated values²⁰⁻²² independently for each MFRSR UVA spectral channel. We do the fitting iteratively, assuming the AERONET retrieval value of k at 440nm as the initial value. We use the absolute value of diffuse/direct fraction residual, $|dd(\text{calculated}) - dd(\text{measured})|$ as a measure of the goodness of the fit regardless of the actual dd value. In all results below the fit tolerance of 0.01 is assumed.
- 11) After a good fit is achieved, the corresponding value of k along with the AERONET particle size distribution is used to calculate scattering albedo, ω , via Lorentz-Mie code. If the good fit is not achieved we regard the retrieval as unsuccessful and do not include it in the analysis.

Ultimately, this approach allows us to derive statistical distribution (daily and seasonal) of the absolute values and spectral dependence of UV single scattering albedo, ω and absorption optical depth in an urban environment typical for the Eastern part of the US.

4. RESULTS

Since the diffuse irradiance measurements are sensitive to the presence of scattered or broken clouds anywhere in the sky, we originally intended to analyze only completely cloud free conditions. However, this turned out to be too strict a requirement at GSFC site, so later we allowed days with a small amount of scattered clouds (see discussion below). Initially, we selected all CIMEL sky radiance almucantar measurements that were automatically cloud cloud-screened by the AERONET data system³⁰ and only looked at the days when AERONET inversions were available. Next, from these days we manually selected completely cloud-free conditions either in the morning or afternoon, by visual inspection, using all-sky digital images. We also filtered out days in January-March with any partial snow cover. Thus we focused on ~30 cloud-free portions of days between October 1 2002 and April 30 2003, meeting strict cloud-free and snow free criteria.

Figure 2 shows 3-min MFRSR ω_{368} retrievals on October 2, 2002 along with CIMEL ω_{440} retrievals using the almucantar technique²⁵. The τ_{368} varied on that day from the value ~0.5-0.6 in the morning to almost 0.8 in late afternoon (figure 1). The τ absolute values were more than twice as high as the annual climatological values at GSFC¹⁹ due to hazy and humid conditions. The morning conditions were cloud-free, while scattered clouds developed between 16GMT and 20GMT and cleared during late afternoon (figure 1).

Under humid conditions, the AERONET single scattering albedo, ω_{440} values were high ω ~0.97-98, except one particular measurement around local noon time (ω_{440} =0.93 at 1559 GMT). The very close agreement between 2 reference CIMELS (#89 and #94) on Oct 2, 2002 in both ω retrievals (differences ranging from ~0.003 to 0.014) and in

τ (differences <0.005) for the entire morning time period (~ 1230 - 1600 GMT) suggest that measurement noise is not the reason for the trend in ω_{440} derived by AERONET. These instruments are independently calibrated at Mauna Loa and both are calibrated on different dates for sky radiance at the GSFC 6-foot integrating sphere. So, the reason for the CIMEL ω trend is a possible subtle cloud cover influence (not obvious in the CIMEL data in either Angstrom exponent or in sky radiance smoothness, however, the whole hemisphere is not viewed), or related to the inversion algorithm using radiance data with a smaller range of scattering angles as the solar zenith decreases, since only sky radiance data at larger scattering angles are sensitive to aerosol absorption. On the other hand, MFRSR ω retrievals were stable during the day, except systematically low ω values during early morning period, when solar zenith angle exceeded 70° . The reason for morning ω drop may be not perfect cosine response of the MFRSR diffuser (underestimating diffuse irradiance)²² and/or using plane parallel version of the forward radiative transfer code. Therefore, we excluded MFRSR data with solar zenith angles exceeded 70° from the figure. Thus, the two methods of estimating ω are complementary in that the Dubovik and King²⁵ retrieval requires large solar angles, while MFRSR data are more reliable at low solar zenith angles.

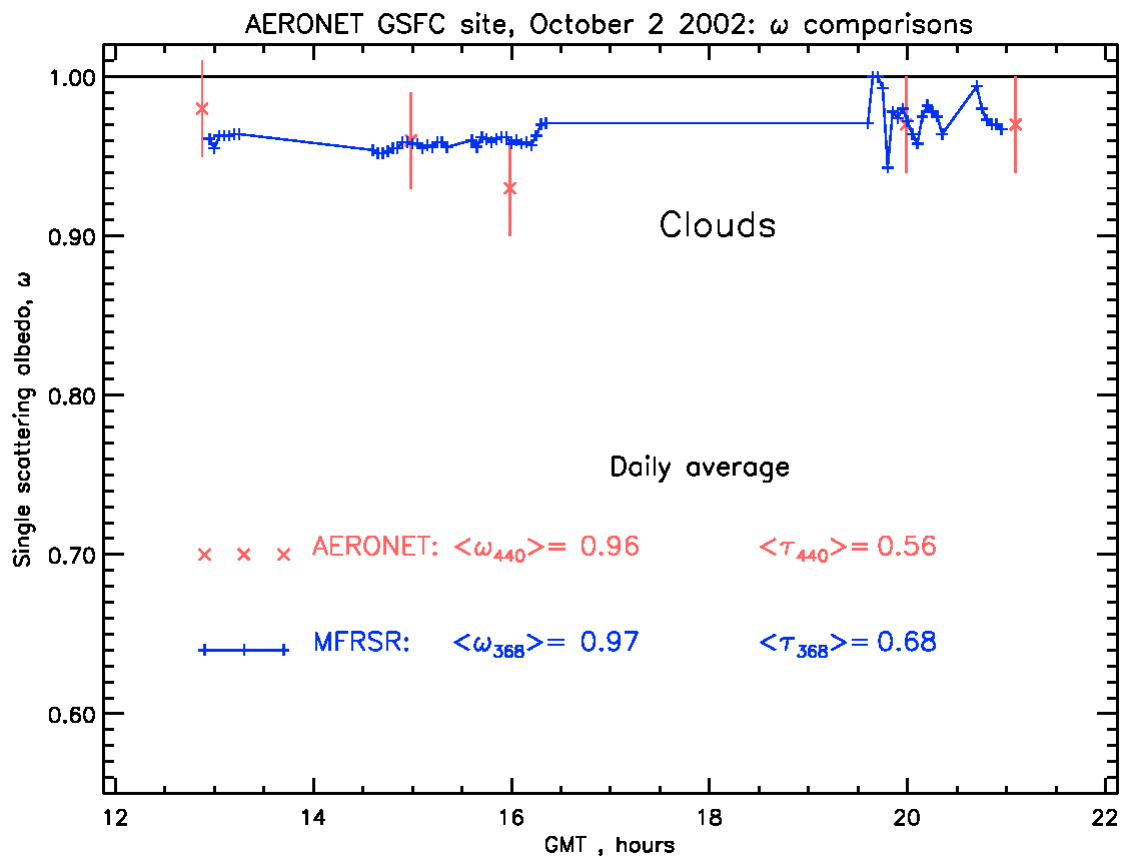


Figure 2. MFRSR and AERONET single scattering albedo retrieval at GSFC on October 2 2002. The 3-minute MFRSR retrieved single scattered albedos at 368nm are shown as small crosses connected with solid line, while AERONET ω retrievals at 440nm are shown as large crosses with ± 0.03 error bars²⁶. The actual solar zenith angle was used in retrieval for each 3-min MFRSR measurement. The forward radiative modeling parameters were: surface albedo 0.02, total ozone 260 Dobson Units, boundary layer aerosol profile and Dubovik and King²⁵ inverted particle size distribution within ± 20 min of each CIMEL almucantar measurement.

We did not find statistically significant spectral variation in ω between 368nm and 325nm on this day. Although MFRSR retrievals suggest ω decreases at shorter UV wavelengths, the difference in ω between 325nm and 368nm is not large (~ 0.02) and is probably within the error bars of the MFRSR ω retrievals¹³. The sensitivity analysis for the Dubovik and King ω algorithm^{25,26}, suggests an uncertainty in ω to be ~ 0.03 at $\tau_{440}=0.5$ and increasing to ~ 0.05 at $\tau_{440}=0.2$ for water-soluble aerosols. Similar analysis needs to be done for MFRSR method before days with low aerosol loadings can be further analyzed.

Clouds present a major challenge for both CIMEL and MFRSR aerosol inversions. Although the AERONET algorithm can filter, to some degree, cloud contaminated sky radiances providing useful aerosol retrievals even for scattered cloud conditions; there is obviously a limit to this capability. This is why no AERONET retrievals were deemed good between 16 GMT and 20 GMT on October 2. When late afternoon cloudiness decreased (figure 1), additional AERONET retrievals were possible with ω values close to the early morning retrievals ($\omega_{440} \sim 0.97-0.98$). Since broken clouds anywhere in the sky affect MFRSR measurements, MFRSR ω retrievals show higher time variability in the afternoon, compared to the morning measurements. When averaged over an hour time period, MFRSR still provides reasonable ω_{368} data (i.e. within 0.02 of AERONET ω_{440} retrievals). Thus, MFRSR ω retrievals may not require completely cloud-free conditions and some degree of scattered clouds can be tolerated as long as clouds do not block the sun. To what degree scattered clouds can be tolerated with MFRSR method requires further investigation.

5. SUMMARY AND DISCUSSION

Combined use of CIMEL sun and sky radiance measurements in the visible with total and diffuse irradiance measurements in UV provide a powerful tool for extrapolating CIMEL visible measurements of column aerosol absorption into UV spectral range. The two methods of estimating ω are complementary in that the Dubovik and King²⁵ retrieval requires large solar angles, while MFRSR data are more reliable at low solar zenith angles. First results of simultaneous and collocated comparisons of the two methods have shown consistent results in ω estimation for large aerosol loadings $\tau_{440} > 0.4$. Application of MFRSR method to days with lower aerosol loadings requires additional accuracy assessment.

Despite different wavelengths and different sensitivity to solar zenith angle and cloudiness ω daily mean values agree well (within AERONET specified error bars $\Delta\omega \sim 0.03$) (figure 2). The daily mean ω values in UV were close to 0.95, which agrees with our previous estimation of ω_{325} for Toronto, CA (see Table 1 and figure 12 from Krotkov et al⁶). Using MFRSR τ_{325} measurements on October 2 (daily average $\langle \tau_{325} \rangle \sim 0.75$), one can further estimate aerosol absorption optical thickness ~ 0.04 at 325nm. This small absorption is difficult to detect using TOMS standard aerosol index method⁶, especially when the aerosol is in the boundary layer (below 2 km). For example, we calculate the TOMS absorbing aerosol index to be negative on this day. As a result, the TOMS UV algorithm would treat the aerosol as non-absorbing⁶ overestimating surface UV(325nm) irradiance by $\sim 10\%$ ¹². Thus, the aerosol absorption alone could explain the average TOMS UV bias found in ground-based comparisons with the Canadian Brewer network¹⁴ and needs to be incorporated in the future versions of the satellite surface irradiance algorithms.

REFERENCES

1. O. Wild, X. Zhu, and M.J. Prather, "Fast-J: Accurate simulation of in- and below-cloud photolysis in tropospheric chemical models", *J. Atmos. Chem.*, **37**, 245-282, 2000.
2. M. Z. Jacobson, "Studying the effects of aerosols on vertical photolysis rate coefficient and temperature profiles over an urban airshed", *Journ. Geophys. Res.*, **103**, 10593-10604, 1998.
3. R.R. Dickerson, S. Kondragunta, G. Stenchikov, K.L. Civerolo, B.G. Doddridge, and B.N. Holben, "The impact of aerosols on solar Ultraviolet radiation and photochemical smog", *Science*, **28**, 827-830, 1997.

4. S. Madronich, *Environmental Effects of Ultraviolet (UV) Radiation*, chapter: UV radiation in the natural and perturbed atmosphere, *Lewis Publisher*, Boca Raton, 17-69, 1993.
5. M. Z. Jacobson, "Isolating nitrated and aromatic aerosols and nitrated aromatic gases as sources of ultraviolet light absorption", *Journ. Geophys. Res.*, **104**, 3527-3542, 1999.
6. N.A. Krotkov, P.K. Bhartia, J.R.Herman, V.Fioletov and J.Kerr, Satellite estimation of spectral surface UV irradiance in the presence of tropospheric aerosols 1. Cloud-free case, *Journ. Geophys. Res.*, **103**, D8, 8779-8793, 1998.
7. A. Kylling, A. F. Bais, M. Blumthaler, J. Schreder, C.S. Zerefos, and E. Kosmidis, "Effect of aerosols on solar UV irradiances during the Photochemical activity and solar ultraviolet radiation campaign", *Journ. Geophys. Res.*, **103**, 26051-26060, 1998.
8. J. Reuder and H. Schwander, "Aerosol effects on UV radiation in nonurban regions", *Journ. Geophys. Res.*, **104**, 4065-4077, 1999.
9. J.R.Herman, N.Krotkov, E.Celarier, D.Larko, and G.Labow, "The distribution of UV radiation at the Earth's surface from TOMS measured UV-backscattered radiances," *J. Geophys. Res.*, **104**, 12059-12076, 1999.
10. B. N. Wenny, V.K. Saxena, and J.E. Frederick, "Aerosol optical depth measurements and their impact on surface levels of ultraviolet-B radiation", *Journ. Geophys. Res.*, **106**, 17311-17319, 2001.
11. N.A. Krotkov, J.R.Herman, P.K. Bhartia, C. Seftor, Antti Arola, J. Kurola, S. Kalliscota, P. Taalas, I. Geogdzhayev, Version 2 TOMS UV algorithm: problems and enhancements, *Opt. Eng.* **41** (12) , 3028-3039, 2002.
12. N. A. Krotkov, J.R.Herman, P.K.Bhartia, C.Seftor, A.Arola, J.Kurola, P.Taalas, I.Geogdzhayev, A. Vasilkov, OMI surface UV irradiance algorithm, P.Stammes (Ed.), vol. 3, ATBD-OMI_03, version 2, 2002 (http://eosps.gsfc.nasa.gov/eos_homepage/for_scientists/atbd/docs/OMI/ATBD-OMI-03.pdf).
13. J.L.Petters, V.K. Saxena, J.R. Slusser, B.N. Wenny, and S. Madronich, "Aerosol single scattering albedo retrieved from measurements of surface UV irradiance and a radiative transfer model", *Journ. Geophys. Res.*, **108** (D9) 4288, doi:10.1029/2002JD002360, 2003.
14. V. Fioletov, J.B.Kerr, D.I.Wardle, N. Krotkov, J.R. Herman, "Comparison of Brewer ultraviolet irradiance measurements with total ozone mapping spectrometer satellite retrievals", *Opt. Eng.* **41** (12) 3051-3061, 2002.
15. D.S. Bigelow, J.R. Slusser, A. F. Beaubien, and J. R. Gibson, "The USDA ultraviolet radiation monitoring program", *Bull. Amer. Meteor. Soc.*, **79**, 601-615, 1998.
16. L. Harrison, J. Michalsky, and J. Berndt, "Automated Multi-Filter Rotating Shadowband Radiometer: An instrument for Optical Depth and Radiation Measurements", *Appl. Optics*, **33**, 5118-5125, 1994.
17. L. Harrison and J. Michalsky, "Objective algorithms for the retrieval of optical depths from ground-based measurements", *Appl. Optics*, **33**, 5126-5132, 1994.
18. B.N. Holben et al., "AERONET – A federated instrument network and data archive for aerosol characterization", *Remote Sensing Environment*, **66**, 1-16, 1998.
19. B.N. Holben et al., "An emerging ground-based aerosol climatology: Aerosol Optical Depth from AERONET", *Journ. Geophys. Res.*, **106**, 12 067-12 097, 2001.
20. B. M. Herman, S.R. Browning, J.J.DeLuisi, "Determination of the effective imaginary term of the complex refractive index of atmospheric dust by remote sensing: The diffuse-direct radiation method", *J. Atmos. Sciences*, **32**, 918-925, 1975.
21. King, M. and B.M. Herman, "Determination of the ground albedo and the index of absorption of atmospheric particles by remote sensing. Part I: Theory", *J.Atmos. Sciences*, **36**, 163-173, 1979.
22. M. King, "Determination of the ground albedo and the index of absorption of atmospheric particles by remote sensing. Part II: Application", *J.Atmos. Sciences*, **36**, 1072-1083, 1979
23. T. F. Eck, B.N. Holben, I. Slutsker, and Alberto Setzer, "Measurements of irradiance attenuation and estimation of aerosol single scattering albedo for biomass burning aerosols in Amazonia", *J. Geophys. Res.*, **103**, 31865-31878, 1998.
24. T. F. Eck, B.N.Holben, D.E. Ward, O. Dubovik, J.S. Reid, A. Smirnov, M.M. Mukelabai, N.C. Hsu, N.T. O'Neil, and I. Slutsker, "Characterization of the optical properties of biomass burning aerosols in Zambia during the 1997 ZIBBEE field campaign", *Journ. Geophys. Res.*, **106**, D4, 3425-3448, 2001.
25. O. Dubovik and M.D. King, "A flexible inversion algorithm for retrieval of aerosol optical properties from Sun and sky radiance measurements", *J. Geophys. Res.*, **105**, D16, 20673-20696, 2000.
26. O. Dubovik, A. Smirnov, B.N. Holben, M. D. King, Y. J. Kaufman, T. F. Eck, and I. Slutsker, "Accuracy assessments of aerosol optical properties retrieved from Aerosol Robotic Network (AERONET) Sun and sky radiance measurements", *J Geophys. Res.*, **105**, D8, 9791-9806, 2000.

27. O. Dubovik, B.Holben, T.Eck, A. Smirnov, Y. J. Kaufman, M. D. King, D. Tanre, and I. Slutsker, Variability of Absorption and Optical properties of key aerosol types observed in worldwide locations, *J. Atmos. Sciences*, **59**, 590-608, 2002.
28. J. Slusser, et al., "Comparison of column ozone retrievals by use of an UV multifilter rotating shadow-band radiometer with those from Brewer and Dobson spectrophotometers", *Appl. Optics*, **38**, 1543-1551, 1999
29. T.F. Eck, B.N.Holben, J.S.Reid, O.Dubovik, A.Smirnov, N.T.O'Neill, I.Slutsker, and S.Kinne, Wavelength dependence of the optical depth of biomass burning, urban and desert dust aerosols, *Journ. Geophys. Res.*, **104**, 31333-31350, 1999.
30. A. Smirnov, B.N.Holben, T.F.Eck, O.Dubovik, and I. Slutsker, "Cloud screening and quality control algorithms for the AERONET data base", *Rem. Sens. Env.*, 73(3), 337-349, 2000
31. Herman, B. M., T. R. Caudill, D. E. Flittner, K. J. Thome, and A. Ben-David, A comparison of the Gauss-Seidel spherical polarized radiative transfer code with other radiative transfer codes, *Appl. Opt.*, 34, 4563-4572, 1995.
32. J.R. Herman and E. Celarier, "Earth surface reflectivity climatology at 340 to 380 nm from TOMS data," *J. Geophys. Res.*, **102**, 28003-28011, 1997.